

Short vs. Long-term Coordination of Drones: When Distributed Optimization Meets Deep Reinforcement Learning

Chuhao Qin*, and Evangelos Pournaras*

*School of Computing, University of Leeds, Leeds, UK

Abstract—Swarms of smart drones, with the support of charging technology, can provide completing sensing capabilities in Smart Cities, such as traffic monitoring and disaster response. Existing approaches, including distributed optimization and deep reinforcement learning (DRL), aim to coordinate drones to achieve cost-effective, high-quality navigation, sensing, and recharging. However, they have distinct challenges: short-term optimization struggles to provide sustained benefits, while long-term DRL lacks scalability, resilience, and flexibility. To bridge this gap, this paper introduces a new progressive approach that encompasses the planning and selection based on distributed optimization, as well as DRL-based flying direction scheduling. Extensive experiment with datasets generated from realistic urban mobility demonstrate the outstanding performance of the proposed solution in traffic monitoring compared to three baseline methods.

Index Terms—Drones, unmanned aerial vehicles, navigation and sensing, charging, distributed optimization, deep reinforcement learning

I. INTRODUCTION

Unmanned Aerial Vehicles (UAVs), referred to as drones, can organize themselves into swarms, fostering collaboration and efficiency in sensor data collection within Smart Cities [1]. With their mobility, autonomy, diverse sensors and the unique vantage view they provide, drones have been widely used in multiple applications, such as reporting traffic violations (e.g., congestion and accidents) at early stage [2], mapping natural disasters [3], measuring air quality [4] and detecting free parking spots [5]. Furthermore, the inherent limitations in battery capacity of drones influence their spatio-temporal coverage. Drones require recharging during long operations with supporting facilities (e.g., charging stations). Recently, scholars have introduced the wireless charging and commercially available charging platforms to enable long-term sensing with drones [6].

Inspired by these studies, this work tackles the problem of coordinating swarms of drones for improved sensing and recharging. The goal is to enhance sensing quality in a large-scale area using both drones and charging stations while minimizing overall costs. Achieving this requires a highly adaptive algorithm for optimizing drone operations. Previous work [7] employed distributed optimization methods for efficient drones path planning and task assignment

to enhance sensing. These methods enable drones to autonomously organize and assign tasks collectively, avoiding centralized decision-making and adapting to the dynamic environment. However, they encounter issues with iterative sensing. In this challenge, the navigation and sensing of drones are significantly influenced by two factors: their flying directions and future sensor data on the map. For example, if drones have information about the expected increase in traffic flow in certain areas, even if those areas are currently sparsely populated with vehicles, they can strategically choose to fly to those locations. This decision can be more profitable for tasks like vehicle detection, despite not providing short-term returns. To clarify, the concept here is akin to "Slower is Faster". Instead of prioritizing quick gains, a long-term planning approach is required to optimize the overall effectiveness and efficiency of drone sensing operations.

Deep reinforcement learning (DRL) tackles the challenge of long-term optimization. It accounts for long-term actions through the Bellman equation, which considers the discounted cumulative reward of behaviors (or actions) [8]. Drones, as heterogeneous agents with distinct behavior patterns and action spaces, can benefit from the powerful deep neural networks employed in DRL, enabling an effective handling of sophisticated state space and time-varying environments. Nevertheless, the curse of dimensionality restricts drones' sensing capabilities to small-scale applications as the number of drones and time periods increase. One approach to mitigate this limitation of scalability is to use a centralized model [9], which performs collaborative scheduling on the behaviors of all agents. However, this approach is centralized and does not provide drones with privacy and autonomy to self-assign their sensing tasks. As a result, drones become less flexible and adaptive to real-time environmental changes, and the system's resilience is compromised, making it susceptible to single points of failure.

Given the aforementioned challenges, there is an opportunity for distributed optimization and DRL to leverage each other's strengths and mitigate their respective weaknesses. Therefore, in this paper, we design a new framework named as the decentralized coordination of planning based on deep reinforcement learning (*DO-RL*). This framework involves a novel multi-agent DRL algorithm that builds upon on a collective learning approach known for its remarkable

Corresponding author: Evangelos Pournaras (email: e.pournaras@leeds.ac.uk).

performance in terms of the scalability (support of a large number of software agents), efficiency (low communication and computational cost), decentralization and resilience [10]–[12]. *DO-RL* relies on a learning model to determine the drones’ strategic flying directions for sensing, which also determines the recharging stations, while leaving the planning and selection of specific sensing operations to a distributed optimization method. This approach significantly reduces the computational complexity of agents, facilitates efficient information sharing, and maintains the privacy and autonomy of each agent to independently decide its navigation and sensing actions. Furthermore, a set of auxiliary approaches is introduced, including a plan generation strategy that provides high-quality and diverse options for drones navigation and sensing, as well as a periodic state update. To evaluate the effectiveness of *DO-RL*, this paper conducts extensive analytical assessments and simulations, comparing it against state-of-the-art baseline methods.

The contributions of this paper are outlined as follows:

- 1) The first attempt to solve the decentralized iterative sensing and recharging problem by coordinating a swarm of interactive drones.
- 2) A progressive approach, *DO-RL*, by integrating both distributed optimization and deep reinforcement learning methods.
- 3) A decentralized planning and selection using multi-agent collective learning to improve scalability, resilience and flexibility.
- 4) A novel DRL algorithm for scheduling drones to optimize their flight directions and recharge strategies, ultimately enhancing sustained sensing performance.
- 5) Insights of extensive experiments using realistic transportation and real-world network to validate the superior performance of the proposed approach over three baseline methods.
- 6) An open source of the proposed approach and an open datasets [13] containing all plans of the studied scenario. They can be used as benchmarks to encourage further research on this problem.

TABLE I
COMPARISON TO RELATED WORK: (✓) INDICATES CRITERIA COVERED, (✗) INDICATES CRITERIA NOT COVERED.

Criteria	Ref.:	[14]	[15]	[16]	[17]	[18]	[19]	[20]	This paper
Decentralization		✓	✓	✓	✗	✓	✗	✗	✓
Long-term efficiency		✗	✗	✗	✓	✓	✓	✓	✓
Iterative sensing		✗	✗	✗	✓	✓	✓	✓	✓
Recharging assignment		✗	✗	✗	✗	✗	✓	✗	✓
Scalability		✗	✗	✓	✗	✗	✗	✗	✓
Resilience		✗	✗	✓	✗	✗	✗	✗	✓
Flexibility		✓	✓	✓	✗	✗	✗	✗	✓

II. RELATED WORK

Sensing task assignment. The UAV task assignment problem for spatio-temporal sensing has been traditionally defined as a combinatorial optimization problem, resembling the Traveling Salesmen Problem [7], [21]. This involves

finding the optimal assignment of tasks to drones at specific locations, while considering constraints such as task urgency, time scheduling, and flying costs. The digraph-based methods, such as greedy approach, [22] particle swarm optimization [23], genetic programming [24] and wolf pack search [25], are introduced to formulate the problem of reaching optimal sensing efficiency in terms of coverage, inspection delay, events detection rate and the cost of flying trajectories. However, these works lack comprehensive evaluation in complex sensing scenarios, such as varying time periods, charging stations, and different sensing distributions. Besides, these centralized methods suffer from a risk of single points of failure [26], wherein the failure of a central control station can lead to system disruptions without autonomous recovery mechanisms.

Distributed optimization. Several distributed task assignment algorithms have been proposed to address the challenges of multi-UAV systems in complex sensing scenarios. One such algorithm is the robust decentralized task assignment (RDTA) [14] that enhances robustness and reduces communication costs by employing decentralized planning for drones. Another algorithm is the consensus-based bundle algorithm (CBBA) [15], which combines market-based mechanisms and situation awareness to converge and avoid task conflicts among drones. Furthermore, a planning-based coordination method using collective learning, named Economic Planning and Optimized Selections (EPOS), enables drones to optimize their navigation and sensing options under battery constraints [16], [27]. However, long-term sensing scenarios poses challenges. Drones tend to prioritize immediate maximum returns in the short term, often overlooking the need for strategic decision-making regarding iterative sensing and recharging.

DRL-based drone sensing. Addressing the drone sensing problem with complex optimization objectives, limited energy consumption, and a large number of heterogeneous agents, the deep reinforcement learning (DRL) algorithm proves to be effective. Liu *et al.* [28] proposed a cooperative DRL-based task allocation strategy for heterogeneous drones that considers the uncertainty of dynamic tasks and has high scalability. Ding *et al.* [17] integrated the mobile crowdsensing (i.e., human equipped with mobile sensing devices such as smartphones) into UAV sensing, which overcomes the limitations of both human mobility and drone battery capacity. Nevertheless, these centralized approaches lack privacy and autonomy for drones in self-assigning tasks, reducing flexibility, adaptability to the real-time changes and increasing vulnerability to single points of failure. Omoniwa *et al.* [18] presented a decentralized approach that leverages DRL and explicitly-communicated information from neighbors to improve the energy efficiency of drones in providing wireless connectivity to ground users in dynamic environments. However, it solves a different problem and is confined to a small number of drones and time periods.

Recharging assignment. Earlier work [29], [30] has studied the recharging scheduling problem: drones efficiently collect sensor data while charging from stations. However, scalability

ity becomes a challenge since the algorithms used in these works only deal with a small number of drones. Zhao *et al.* [19] proposed a comprehensive solution for sustainable urban-scale sensing in open parking spaces, specifically for detecting available parking spots. Their solution incorporates the task selection and scheduling using DRL, and adaptive charging scheduling. However, these methods are centralized and tailored exclusively to the sensing scenario of open parking spaces.

Transportation application. Despite the potential of drones in improving traffic monitoring accuracy, safety, and cost savings, there is limited research focused on task assignment in this particular scenario. Elloumi *et al.* [31] proposed a road traffic monitoring system that generates adaptive drones trajectories by extracting information about vehicles. Huang *et al.* [32] developed the pre-flight conflict detection and resolution method, where service providers of drones with their own interest can coordinate to address the path planning problem. Samir *et al.* [20] leveraged DRL algorithm to optimize the trajectories of UAVs, with the objective of minimizing the age of information of collected data. While these approaches demonstrate high performance in the detection of traffic vehicles, they do not explicitly address the challenges of iterative sensing and recharging. Furthermore, they assume prior knowledge of the traffic flow of the vehicles, which may not be readily available in practical scenarios.

In summary, this paper bridges a gap in previous approaches. It empowers drones not only to make strategic choices in flying directions and recharging locations by predicting traffic flow but also enables them to autonomously optimize their sensing operations in a decentralized manner.

III. FRAMEWORK OVERVIEW

In this section, we introduce the designed framework to solve the decentralized iterative sensing and recharging problem by a swarm of drones. Table II illustrates the list of mathematical notations used in this paper.

A. Scenario and Modeling

Sensing map. Consider a swarm of drones $\mathcal{U} \triangleq \{1, 2, \dots, U\}$ performing sensing missions, such as monitoring vehicles, over a grid that represents a 2D map. In this scenario, a set of grid cells (or points of interest) $\mathcal{N} \triangleq \{1, 2, \dots, N\}$ are uniformly arranged to cover the map. The primary goal of the drones is to coordinate their visits to these cells to collect the required data. Furthermore, a set of charging stations $\mathcal{M} \triangleq \{1, 2, \dots, M\}$, from which the drones depart from and return to, are located at fixed coordinates on the map.

Time periods and slots. We assume a set of time periods as $\mathcal{T} \triangleq \{1, 2, \dots, T\}$. Each time period can be divided into a set of equal-length scheduling timeslots $\mathcal{S} \triangleq \{1, 2, \dots, S\}$. In each timeslot, a drone can be controlled to fly to a cell and hover to collect sensor data.

Matrix of plans. To explain the short-term navigation and sensing of drones over the cells and timeslots in a period

TABLE II
NOTATIONS.

Notation	Explanation
u, U, \mathcal{U}	The index of a drone; the total number of drones; the set of drones
m, M, \mathcal{M}	The index of a charging station; the total number of charging stations; the set of charging stations
n, N, \mathcal{N}	The index of a grid cell; the total number of grid cells; the set of grid cells
s, S, \mathcal{S}	The index of a timeslot; the total number of timeslots in a period; the set of timeslots
t, T, \mathcal{T}	The index of a period; the total number of periods; the set of periods
a^u	The period-by-period action taken by u
$\mathcal{A}^u, \alpha_{n,s}^u$	The plan of u ; the plan of u at cell n and timeslot s
$\mathcal{A}, \alpha_{n,s}$	The aggregated plan of all drones; the aggregated plan at cell n and timeslot s
$\mathcal{R}, r_{n,s}$	The target; the target at cell n and timeslot s
$V_{n,s}$	The required sensing value at cell n and timeslot s
$V'_{n,s}$	The overall sensing value collected by all drones at cell n and timeslot s
$\hat{V}_{n,s}$	The predicted sensing value at cell n and timeslot s
p^{a^u}	The group of generated plans when u take action of a^u
l, L	The index of a plan in p^{a^u} ; the total number of plans in p^{a^u}
P_u^f, t_u^f	The flying power consumption of u ; the flying time
P_u^h, t_u^h	The hovering power consumption of u ; the hovering time
J^u, K^{a^u}	The number of visited cells (mobility range) of u ; the range for u selecting visited cells
β	The behavior of an agent in planning optimization
c^u, e^u	The current location of u ; the current energy consumption of u
o_t^u, r_t^u	The observation of u at the period t ; the reward of u at the period t
k, H	The index of a sampled transition; the number of sampled transitions; the clip interval hyperparameter
γ, ϵ	The clip interval hyperparameter; the discount factor
$Q(\cdot), \theta^\pi$	The critic network; the parameter of critic network
$\pi(\cdot), \theta^\pi$	The actor network; the parameter of actor network
$\omega_{n,s}, \bar{v}$	The prediction coefficient to calculate $\hat{V}_{n,s}$; the threshold to remove the regions with low sensing requirements

$t, t \in \mathcal{T}$, the plans of drones $\{\mathcal{A}^1(t), \mathcal{A}^2(t), \dots, \mathcal{A}^U(t)\}$ are introduced. Each plan is encoded by a matrix with the size of $N \times S$, with each element represented as $\alpha_{n,s}^u(t) \in \{0, 1\}$. Here, $\alpha_{n,s}^u(t) = 1$ denotes the drone u hovers and collects all data at the cell n at timeslot s , whereas $\alpha_{n,s}^u(t) = 0$ denotes the drone does not hover at the cell at that time.

Action. To explain the long-term navigation and sensing over all periods, we introduce the period-by-period actions of each drone $a^u = \{0, 1, 2, \dots, 9\}$, meaning to control u to move horizontally along eight directions, which are 1 = north (N), 2 = east (E), 3 = south (S), 4 = west (W), 5 = northeast (NE), 6 = southeast (SE), 7 = southwest (SW), and 8 = northwest (NW), or return to the origin ($a^u = 0$). Under each action, u executes a plan $\mathcal{A}^u(t)$. After completing its sensing tasks, u flies back to one of the charging stations to recharge fully and resume work in the next period $t + 1$.

Matrix of aggregated plan. The matrix of the aggregated plan is defined as $\mathcal{A}(t) = \{\alpha_{n,s}(t)\}$, where the element $\alpha_{n,s}(t)$ denotes whether the cell n in the map is covered by drones at timeslot s in the period t . We assume that when multiple drones cover a cell at the same time, they are regarded as one drone, because they collect the same spatio-temporal sensor data. Thus, the aggregated plan can

be denoted as $\alpha_{n,s}(t) = \min(\sum_{u=1}^U \alpha_{n,s}^u(t), 1)$.

Matrices of required and collected data. In the context of a sensing task, each cell at a timeslot has specific sensing requirements that determine the data acquisition of drones. Such sensing requirements can be determined by city authorities as a continuous kernel density estimation, for example, monitoring cycling risk based on requirements calculated by past bike accident data and other information [16], [33]. The high risk level of a cell at a timeslot represents the high importance of sensing (e.g., the crucial intersection of traffic flow), and thus a high number of required sensing values is set. The matrix of required sensing values is denoted as $V(t) = \{V_{n,s}(t)\}$, and the matrix of overall sensor data collected by all drones as $V'(t) = \{V'_{n,s}(t)\}$, where $V_{n,s}(t)$ and $V'_{n,s}(t)$ denote the required and collected value at cell n and timeslot s respectively. Noted that drones can collect all required data of a cell within a timeslot, and thus $V'(t) = \mathcal{A}(t) \circ V(t)$, where \circ represents the element-wise product of two matrices.

Matrix of target. In a real-world scenario, drones lack prior knowledge of the amount of required data values before they begin their sensing operations. Therefore, it becomes essential to build a target that instructs the drones regarding when and where they should or should not fly to. The matrix of the target is defined as $\mathcal{R}(t)$, which denotes the sensing requirements for all drones in the period t . The element of target is denoted as $r_{n,s}(t) = \{0, 1\}$, $n \in \mathcal{N}$, $s \in \mathcal{S}$, where $r_{n,s}(t) = 1$ requires only one drone to visit the cell n at timeslot s , and $r_{n,s}(t) = 0$ prohibits any drones collecting sensor data.

Assumptions. To simplify the scenario, this paper makes the following assumptions: 1) Each drone is programmed to fly at a unique altitude while moving between cells to prevent collisions. 2) Each time period concludes a flying period and a charging period: one is the time that drones perform sensing, while the other is for charging. All drones finish charging before the next time period begins. 3) Each charging station is adequately equipped with charging capacity, enabling multiple drones to charge simultaneously without the need for queuing. This arrangement prevents any delays in the charging process.

B. Problem Formulation

We model the scenario of a swarm of drones that perform sensing by considering the following performance metrics: 1) mission efficiency; 2) sensing accuracy; and 3) energy cost.

Mission efficiency. It denotes the ratio of sensing values in all cells at all timeslots collected by the drones during their mission over the total required values in all cells at all timeslots during the period t . It is formulated as:

$$\text{Eff}(\mathcal{A}^u, t) = \frac{1}{U} \cdot \frac{\sum_{n=1}^N \sum_{s=1}^S V'_{n,s}(t)}{\sum_{n=1}^N \sum_{s=1}^S V_{n,s}(t)}. \quad (1)$$

Sensing accuracy. It denotes the matching (or correlation¹) between the total sensing values collected and the required ones. The metric is formulated as follows:

$$\text{Acc}(\mathcal{A}^u, t) = \frac{1}{U} \cdot \sqrt{\frac{N * S}{\sum_{n=1}^N \sum_{s=1}^S (V'_{n,s}(t) - V_{n,s}(t))^2}}. \quad (2)$$

Energy cost. It is the energy consumed by drones to perform spatio-temporal sensing. A power consumption model [34] is used to calculate the power consumption with input the specification of drones (weight, propeller and power efficiency). This model estimates the cost of navigation and sensing plans, and helps to emulate the outdoor environments [16]. The energy cost of each drone u is formulated as:

$$E(\mathcal{A}^u, t) = P_u^f \cdot t^f(\mathcal{A}^u) + P_u^h \cdot t^h(\mathcal{A}^u), \quad (3)$$

where P_u^f and P_u^h are the flying and hovering power consumption of drone u respectively; t^f and t^h are the flying and hovering time respectively, which are determined by the sensing plans \mathcal{A}^u during the period t .

Overall performance. The optimization problem has three objectives: 1) maximize mission efficiency; 2) maximize sensing accuracy; and 3) minimize energy cost. Simultaneously achieving all of these objectives is a daunting task, as they are often opposing to each other. Maximizing both efficiency and accuracy is a tradeoff since increasing efficiency of mission results in sensing imbalance and even blind areas by under-sensing. In addition, in order to achieve both of these goals, drones have to continuously move to collect data from different cells, which results in higher energy costs due to long-distance movements. However, some movements of drones may not improve the sensing quality in the long run. For instance, at the end of a period, drones opt to return to the nearest charging station where there are fewer sensing tasks in the next period. This choice reduces the energy cost of the current period but comes at the significant expense of sacrificing the sensing quality in the next period. Therefore, the overall sensing performance is optimized by integrating these contradictory objectives and finding the plans of each drone over all time periods. The objective function is formulated as follows:

$$\arg \max_{\mathcal{A}^u, u \in \mathcal{U}} \sum_{u=1}^U \sum_{t=1}^T [\text{Eff}(\mathcal{A}^u, t) \cdot \text{Acc}(\mathcal{A}^u, t) - E(\mathcal{A}^u, t)]. \quad (4)$$

C. Framework Overview

For high-quality sensing performance, the proposed approach relies on both decentralized drone coordination for short-term navigation and sensing optimization, as well as long-term scheduling of flight directions to adapt to changing environments. Fig.1 illustrates the designed system framework of *DO-RL*, consisting of four main components:

¹Error and correlation metrics such as the root mean squared error, cross-correlation or residuals of summed squares can estimate the matching, which is shown earlier to be an NP-hard combinatorial optimization problem in this context [10], [11].

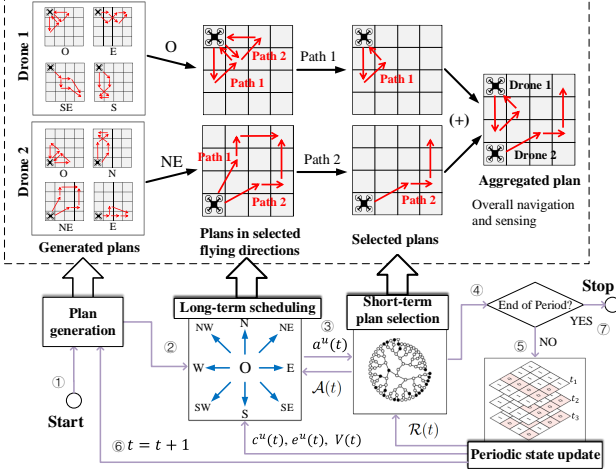


Fig. 1. System framework of DO-RL.

Initialization plan generation. This component generates the navigation and sensing options for drones. Given the sensing map, each drone, controlled by a local software agent, autonomously generates a finite number of discrete plans at the beginning of the process. This provides flexibility for the drones to choose in a coordinated way. The generated plans are grouped into different flying directions.

Short-term plan selection. This component coordinates drones to select the optimal navigation and sensing options from their generated plans within a period. It outputs the aggregated plan $\mathcal{A}(t)$ shared to all drones.

DRL-based long-term scheduling. This component is the core of the framework, which leverages the DRL algorithm to enable drones to take their period-by-period actions a^u (N, E, S, W, NE, SE, SW, NW or O) based on the distribution of sensor data values. Specifically, drones determine their flying directions with the highest sensor data values over all periods. Then, the generated plans with the corresponding actions are chosen for the short-term plan selection. Note that drones return to the nearest charging stations after sensing, and depart from them in the next period.

Periodic state update. This component updates the state of drones (i.e., the current location $c^u(t)$ and energy cost $e^u(t)$) and the system (i.e., the target $\mathcal{R}(t)$ and required sensor data values $V(t)$) for the long-term scheduling in the next period.

IV. DETAILED DESIGN OF FRAMEWORK

A. Initialization Plan Generation

Each drone generates nine groups of plans, each associated with an action for a flying direction, and these groups comprise multiple individual plans. Consequently, drones can adjust their assignments as condition changes, more flexible and adaptive to the dynamic environment. A group of plans generated by drone u during a period is defined as $p^{a^u}(t)$, where each plan in the group have the same action. A plan with index of l is denoted as $\mathcal{A}_l^u(t)$, $l \leq L$,

$\mathcal{A}_l^u(t) \in p^{a^u}(t)$, where L denotes the total number of plans in a group. Therein, each plan has sensing information about the path specifications of the drone, such as the visited cells, the timing of data acquisition over these cells, and the corresponding (normalized) energy consumption. Thus, we define $\mathcal{A}_l^u(t) = \{\mathcal{A}_l^u(t) | E(\mathcal{A}_l^u)\}$, where $\mathcal{A}_l^u(t)$ indicates the visited cells and hovering time; $E(\mathcal{A}_l^u)$ denotes the energy consumed by u traveling over these visited cells, i.e., the cost of the plan.

Path finding and energy calculation. A drone generates a plan by determining its optimal path and calculating the energy required for traversing that path. For example of a plan $\mathcal{A}_l^u(t) \in p^{a^u}(t)$, the drone u finds a total number of J^u visited cells randomly from a range of cells K^{a^u} . This range is calculated based on the departure of u and its action for a flying direction a^u ; the cells close to this direction. Then, u finds the shortest possible path among these J^u cells, departure and destination via the *greedy algorithm* for Traveling Salesmen Problem. The path includes the information that which cell and which timeslot the drone collects data, and thus both the traveling time $t^f(\mathcal{A}_l^u)$ and hovering time $t^h(\mathcal{A}_l^u)$ are calculated. The total energy consumption $E(\mathcal{A}_l^u)$ when u travels over the path is then calculated via Eq.(3).

B. Short-term Plan Selection

Given the generated plans in a period, the agent of each drone connects into a tree communication structure, as shown in Fig. 1, within which it interacts with its children and parent in a bottom-up and top-down fashion to improve plan selections iteratively [10]. Specifically, each agent obtains the aggregated choices from other agents via interaction, and chooses one of the plans $\mathcal{A}_l^u(t)$ such that all choices together $\mathcal{A}(t) = \sum_u \mathcal{A}_l^u(t)$ add up to match a target $\mathcal{R}(t)$. The target is used to direct a single drone to sense in a cell during a timeslot, thereby avoiding the simultaneous sensing of multiple drones within the same cell.

The purpose is to match the aggregated plans $\mathcal{A}(t) = \{\alpha_{n,s}(t)\}$ to the target $\mathcal{R}(t) = \{r_{n,s}(t)\}$. Two opposing objectives are minimized: the average difference between $\mathcal{A}(t)$ and $\mathcal{R}(t)$, as well as the energy cost of the plan selected by the drone $E(\mathcal{A}_l^u)$. The cost function for each agent is formulated based on the root mean square error (RMSE), shown as follows:

$$\min_{\mathcal{A}_l^u, u \in \mathcal{U}} (1 - \beta) \sqrt{\frac{\sum_{n=1}^N \sum_{s=1}^S (\alpha_{n,s}(t) - r_{n,s}(t))^2}{N * S}} + \beta E(\mathcal{A}_l^u), \quad (5)$$

where β represents the behavior of an agent. As the value of β increases, the agent becomes increasingly selfish, prioritizing plans with lower energy costs at the expense of higher root mean squared error. Each agent (or drone) aims to minimize the system-wide cost of sensing while considering its energy consumption. However, drones need adaptability in accomplishing dynamic missions in response to a changing environment. In the proposed approach, long-term actions enable drones to focus their efforts on areas

with abundant sensor data, enhancing their efficiency in navigation and sensing.

C. DRL-based Long-term Scheduling

The process of determining actions for drones is hindered by what is commonly known as the "dimensional curse." This curse arises exponentially as the increase in the number of drones, cells and time periods, which escalates the complexity of the scheduling problem. Furthermore, the complex distribution of sensor data values on the map further enhances the difficulty in scheduling effectively the actions for the drones. To tackle these issues, the proposed method incorporates the deep reinforcement learning algorithm.

DRL Modeling. We model the problem using state, action, and reward concepts.

(1) *State*: The state \mathbf{s}_t in period t consists of four components ($\mathcal{S}_1, \mathcal{S}_2, \mathcal{S}_3, \mathcal{S}_4$).

- $\mathcal{S}_1 = \{c^1(t), \dots, c^U(t)\}$: current locations of all drones. Since drones charge at charging stations before taking actions, the location can serve as the index of charging station, $c^u(t) = m$.
- $\mathcal{S}_2 = \{e^1(t), \dots, e^U(t)\}$: current energy consumption of all drones.
- $\mathcal{S}_3 = \{\alpha_{1,1}(t), \dots, \alpha_{n,s}(t), \dots, \alpha_{N,S}(t)\}$: the aggregated plan of all drones.
- $\mathcal{S}_4 = \{V_{1,1}(t), \dots, V_{n,s}(t), \dots, V_{N,S}(t)\}$: the required distribution of sensor data values.

(2) *Action*: The action $\mathbf{a}_t = \{a_t^1, \dots, a_t^U\}$ in period t consists of flying directions of all drones.

(3) *Reward*: Based on the objective function Eq.(4), the expected immediate local reward of one agent at period t is defined as follows:

$$\mathbf{r}_t^u = \text{Eff}(t) \cdot \text{Acc}(t) - E^u(t), \quad (6)$$

where the first part includes the mission efficiency and sensing accuracy calculated via Eq.(1) and (2), the second part is the energy cost of drone u calculated via Eq.(3).

Global observation. To mitigate expanded state space and achieve better collaborative scheduling, we design a global observation where each drone evaluates an immediate reward based on the aggregated information of all drones. Based on the tree communication structure built in the short-term planning, the agents of drones aggregate and upload their states in a bottom-up fashion, including the aggregated plan and the required sensor data values, and obtain the shared states in a top-down process [10]. The advantages of the global observation are listed as follows:

- Due to the tree structure, the coordination among agents is highly-efficient with low computational and communication cost [10].
- Since agents share the aggregated states instead of the agents one, a single compromised agent is challenging to affect the actions of other agents, which make the system more resilient to attacks or failures [35].
- Each agent is flexible and can choose its own path to navigate among sensing cells and charging stations without over-relying on the policies of other agents.

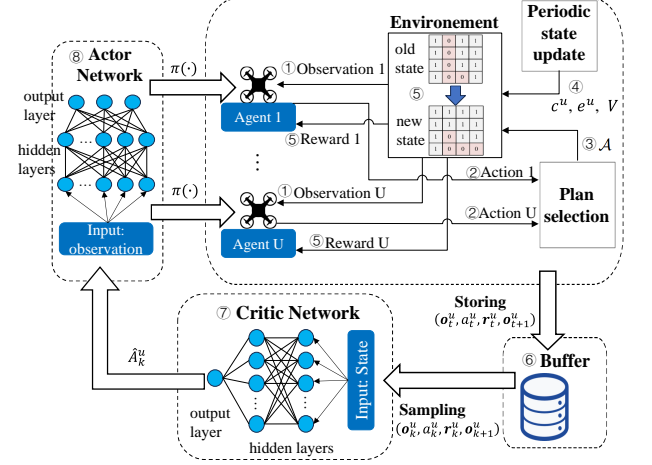


Fig. 2. DRL-based long-term scheduling overview.

Centralized critic multiple actors. Our approach provides a generalized model for multi-agent reinforcement learning with one centralized critic and multiple actors. The actors allow drones to work independently and choose actions based on their observations and policies, allowing for parallel data collection and processing. The centralized critic, however, evaluates the joint actions of drones and guide them toward collectively optimal decisions. As a result, this design enhances the model's robustness, adaptability, and coordination capabilities in complex environments. In addition, the proposed method employ Proximal Policy Optimization (PPO) to prevent detrimental updates and improving the stability of the learning process [36].

Analysis on centralization and decentralization. We assume that there is an authority that control the iterative flying directions of drones using deep reinforcement learning. This entity instructs the drones on which charging station they should return to at the end of their current flight period and depart from at the commencement of the next. Besides, these drones are owned by various entities, including aviation agencies, private citizens, and companies. They engage in a cooperative effort to establish their own unique navigation and sensing strategies, along with corresponding energy consumption plans. Significantly, these strategies are based on the collective sum of all plans rather than individualized, private sensing information. As a result, the governing authority does not exert any influence over the decision-making process regarding the sensing behaviors of the drones. This approach carries significant benefits, particularly in terms of privacy preservation and resilience. It ensures that even in the event of an attack on the governing authority, the drones can maintain their operational integrity.

Overall framework. Fig. 2 illustrates the overall framework of the DRL-based long-term scheduling. The process primarily involves the following steps: Firstly, each agent takes an action for a flying direction based on the global observation \mathbf{o}_t^u shared through coordination as well as the

reward \mathbf{r}_t^u . This observation contains various information of a drone: its current location, energy consumption, the aggregated plan and required sensor data values. Once all actions are determined, drones select their plans and transition to a new state. Subsequently, the buffer, a data storage structure used for experience replay, stores all transitions of each agent $(\mathbf{o}_t^u, \mathbf{a}_t^u, \mathbf{r}_t^u, \mathbf{o}_{t+1}^u)$. Several groups of transitions $(\mathbf{o}_k^u, \mathbf{a}_k^u, \mathbf{r}_k^u, \mathbf{o}_{k+1}^u)$ are sampled randomly (H groups of transitions) for updating the parameters of both the critic and actor networks. The algorithm is typically an extension of the actor-critic policy gradient approach, employing two deep neural networks for each agent: a critic network $Q(\cdot)$ and an actor network $\pi(\cdot)$. The critic network estimates the reward associated with a transition using Bellman equation, and its parameter θ^Q is then updated by minimizing a loss function $L(\theta^Q)$:

$$L(\theta^Q) = \frac{1}{H \cdot U} \sum_{k=1}^H \sum_{u=1}^U (\hat{A}_k^u)^2, \quad (7)$$

$$\hat{A}_k^u = \mathbf{r}_k + \gamma Q(\mathbf{o}_{k+1}^u, \mathbf{a}_{k+1}^u) - Q(\mathbf{o}_k^u, \mathbf{a}_k^u), \quad (8)$$

where γ is a discount factor; \hat{A}_k^u is an advantage function. Then, the critic network provides \hat{A}_k^u to the actor network to increase the probability of actions that have a positive advantage and decrease that have negative advantage. The actions will be taken by drones as $\mathbf{a}_t^u = \pi(\mathbf{o}_t^u)$. The parameter of actor network θ^π is updated by maximizing the clip objective $L_{CLIP}(\theta^\pi)$, as [36]:

$$L_{CLIP}(\theta^\pi) = \frac{1}{H \cdot U} \sum_{k=1}^H \sum_{u=1}^U \min(\text{ratio}(\theta^\pi, u), \text{clip}(\text{ratio}(\theta^\pi, u), 1 - \epsilon, 1 + \epsilon) \hat{A}_k^u), \quad (9)$$

$$\text{ratio}(\theta^\pi, u) = \frac{\pi(\mathbf{a}_k^u | \mathbf{o}_k^u)}{\pi_{old}(\mathbf{a}_k^u | \mathbf{o}_k^u)}, \quad (10)$$

where ϵ is a hyperparameter; $\text{clip}(\cdot)$ defines the surrogate objective by limiting the range of $\text{ratio}(\cdot)$ using clipping, thereby eliminating incentives to exceed the interval $[1 - \epsilon, 1 + \epsilon]$; π_{old} denotes the older policy of the actor network in the previous iteration.

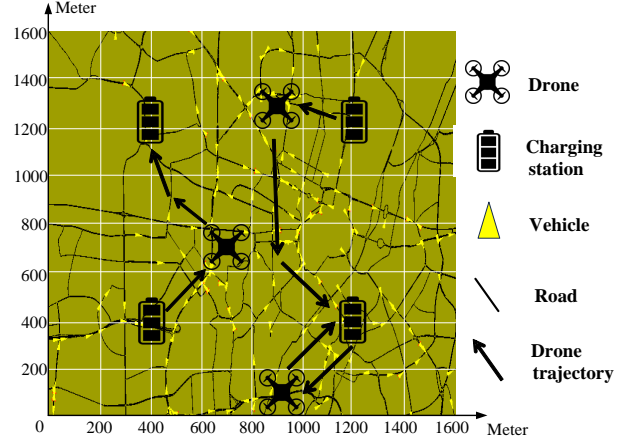
D. Periodic State Update

Location and energy. Each drone changes its location at the next period $t+1$ as $\mathbf{c}_{t+1}^u = \mathbf{a}_t^u$. Given the selected plan \mathcal{A}^u , u updates its current energy consumption as $e_{t+1}^u = E(\mathcal{A}^u, t)$.

Predicted sensor data. Due to evolving environmental conditions, drones have no knowledge about the required values of sensor data in the next period. Thus, the predicted sensor data \hat{V} is used to estimate the required one V based on the historical information. The $\hat{V}(t)$ at period t is updated in a time-reverse decay, formulated as follows:

$$\hat{V}_{n,s}(t) = \sum_{t'=1}^t (T - t + t') \cdot \omega_{n,s}(t') \cdot V'_{n,s}(t'), \quad (11)$$

$$V_{n,s}(t) := \hat{V}_{n,s}(t), \quad (12)$$



(a) Basic scenario with 64 cells, 4 charging stations and high density of vehicles.

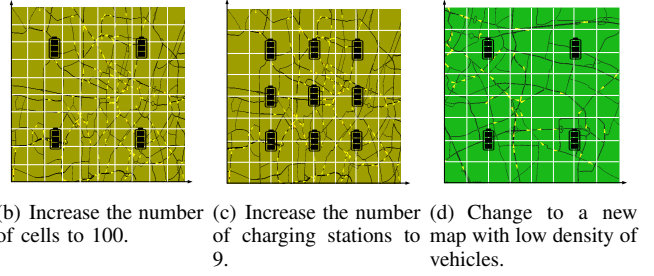


Fig. 3. The central business district of Munich, Germany.

where $V'_{n,s}$ denotes the data values collected by drones once they execute their selected plans (the total collected values are aggregated and shared to each agent via the top-down interactions [10]); $\omega_{n,s}(t')$ is a prediction coefficient such that $0 < \omega_{n,s}(t') < 1$, $t' \leq t$. To achieve accurate predictions, the proposed method leverages the Ordinary Least Squares regression method (OLS) to train these coefficients initially, and use the past experienced observations as the target distribution for training. After that, both current collected data values $V'_{n,s}$ and the predicted one $\hat{V}_{n,s}$ are shared to all agents via the tree communication structure.

Target. The target \mathcal{R} in short-term plan selection needs to be iteratively updated to facilitate drones coordination in choosing plans for areas and timeslots with abundant sensor data. The *trimmed mean* is used to eliminate the extreme low sensing values collected by drones. We initialize the target as $r_{n,s}(0) = 1$ to encompass all cells and timeslots, and update it as follows:

$$r_{n,s}(t) = \begin{cases} 0, & V'_{n,s}(t) < \bar{v} \wedge \alpha_{n,s}(t) > 0 \\ r_{n,s}(t-1), & \text{otherwise} \end{cases}, \quad (13)$$

where the threshold \bar{v} is set iteratively and calculated as the value at the $100(1 - U/N)$ th percentile among the predicted data values $\hat{V}_{n,s}(t)$. Setting the threshold based on the desired percentile removes the need for data collection in those regions with low sensing requirements (e.g., traffic exclusion zones).

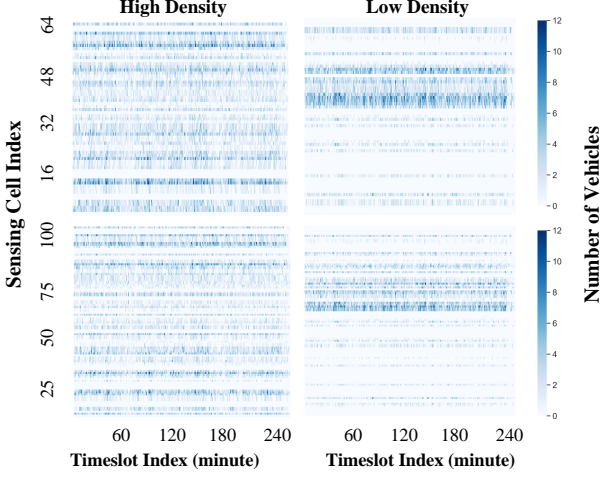


Fig. 4. The distribution of traffic vehicles in the high density area with 64 cells (upper left), high density area with 100 cells (bottom left), low density area with 64 cells (upper right) and low density area with 100 cells (bottom right). All types of areas have 8 periods, each with 30min, which is 240min at total.

V. PERFORMANCE EVALUATION

In this section, an overview of the experimental settings is presented. The sensor dataset, drone's specification, optimization algorithm employed, and neural network used are introduced. Then, the baselines and performance evaluation metrics are discussed. Finally, the simulation results are assessed across various scenarios.

A. Experimental Settings

Scenario model. In order to evaluate the *DO-RL*, we model a real-world transportation scenario, where a swarm of drones perform the sensing tasks of traffic monitoring. The scenario involves a real-world map of Munich city, imported to the simulations of urban mobility (SUMO)² to accurately simulate realistic flows of vehicles. Fig. 3 illustrates a selected map of 1600 × 1600 meters in the city with the simulation time of 100 periods (50 hours). It has a high density of vehicles, approximately 2,000 vehicles passing by per hour. The area split into a finite number of cells, each is defined as a rectangular square with the size of 200 × 200 meters that can be captured by the cameras of drones. The charging stations are uniformly distributed in the map. We employ the cross-validation: 80% simulation time of the datasets for training and 20% for testing. There are two scenarios for the experimental evaluation in this paper:

- *Basic scenario.* It has 64 cells, 4 charging stations and 8 time periods (set as 30min). It has high density of vehicles, around 2,000 vehicles passing by per time period. 16 drones sense the area (camera recording) in parallel. The purpose is to compare different varying parameters in the proposed method.
- *Complex scenario.* It varies the parameter settings such as the density of drones and vehicles, as well as the number

of time periods, cells and charging stations. The goal is to assess the scalability of the proposed method in different experimental conditions.

Drones. We assume that all drones are of the same type, specifically the DJI Phantom 4 Pro model³. Each drone has a body weight of 1.07 kg and four propellers, each with a diameter of 0.35 m. The ground speed of the drones is set at 6.94 m/s, and the drag force is determined to be 4.1134 N [34]. As a consequence, the power consumption remains consistent across all drones. Additionally, drones are equipped with a 6000 mAh LiPo 2S battery (0.31 kg) [37]. The maximum flying time for drones is approximately 30 min, which is set as one flying period. A flying period has $S = 30$ timeslots, each with one minute. To ensure sufficient charging time and prevent drones from delaying their departure in the next iterative sensing, we set the charging period (more details in Appendix B). Moreover, to ensure that the camera covers the entire area of a cell (see Fig. 3), the minimum hovering height of drones is determined at which the field of view of the camera and the cell overlap. The hovering height h is calculated based on the distance between any two cells (approximately 200 meters), the number of pixels, focal length derived from camera calibration, and ground sampling distance [38]. Therefore, each drone equipped with a 4K camera in our study senses from a minimum height of 82.4 meters.

Planning and distributed optimization. We leverage the decentralized multi-agent collective learning method of EPOS⁴, the *Economic Planning and Optimized Selections* [10]. We generate $L = 64$ plans for each agent. All generated plans are made openly available to encourage further research on coordinated spatio-temporal sensing of drones [13], [16], [27]. Each agent in EPOS is mapped to a drone. During the coordinated plan selection via EPOS, agents self-organize into a balanced binary tree as a way of structuring efficient learning interactions [39]. The shared goal of the agents is to minimize the RMSE between the total sensor values collected and the target via Eq.(5), both in unit-length scaled. In the one execution of EPOS, the agents perform 40 bottom-up and top-down learning iterations during which RMSE converges to a minimum optimized value. To minimize the RMSE and the cost of plans, we make an empirical choice of parameters, such as the number of visited cells (mobility range) $J^u = 2$ and the behavior of agents $\beta \in [0.1, 0.8]$. The effect of different parameters is illustrated in Appendix A.

Neural network and learning algorithm. We sample $H = 64$ groups of transitions as minibatches in a replay buffer, and set the discount factor as 0.95 and the clip interval hyperparameter to 0.2 for policy updating. Then we try different multi-layer perceptions (MLP), and use 64 neurons in the three hidden layers of the MLP in both critic and actor networks. The activation function used for the networks is tanh. We train the models for 5000 episodes.

³<https://www.dji.com/uk/phantom-4-pro/info>

⁴EPOS is open-source and available at: <https://github.com/epournaras/EPOS>.

²<https://www.eclipse.org/sumo/>

Complexity. The comparison of both computational and communicational cost is shown in Table III, where I_e denotes the total number of iterations in EPOS; $|S|$ is the number of states, and $|A|$ is the number of actions.

TABLE III
COMPARISON OF COMPUTATIONAL AND COMMUNICATIONAL COSTS.

Attributes	Approaches:	EPOS [10]	MAPPO [17]	DCO-DRL
Computational Cost (agent)		$O(L \cdot I_e)$	$O(S \cdot A)$	$O(L \cdot I_e + S \cdot A)$
Computational Cost (system)		$O(L \cdot I_e \cdot \log U)$	$O(S \times A \cdot U)$	$O((L \cdot I_e + S \cdot A) \cdot \log U)$
Communicational Cost (agent)		$O(I_e)$	$O(1)$	$O(I_e)$
Communicational Cost (system)		$O(I_e \cdot \log U)$	$O(U^2)$	$O(I_e \cdot \log U)$

B. Baselines and Metrics

We compare the *DO-RL* with the following baseline methods:

Greedy. It aims to assign each drone to a single cell, enabling it to accomplish the necessary sensing tasks within a time period [22]. This algorithm minimizes the number of visited cells and travel distance, resulting in reduced energy consumption for drones. To promote decentralization, we implement the algorithm with a local view for each drone, i.e., they have no coordination or awareness of cell occupancy by other drones. By adopting this decentralized approach, we ensure energy-efficient and an independent operation of each drone.

EPOS. It is designed to select the optimal plan for drones based on the generated plans [10]. It incorporates the plan generation and the periodic state update, but does not have the strategic determination in flying directions. Agents randomly choose any charging station to land on at every period.

MAPPO. It is one state-of-the-art DRL algorithm using PPO [36], but does not include distributed optimization compared to *DO-RL*. Another difference lies in that the agents in *MAPPO* learn the flying directions timeslot-by-timeslot, rather than period-by-period in *DO-RL*. At each timeslot, a drone takes actions to horizontally move to an adjacent cell in eight directions (similar to directions shown in Fig. 1) or hover. Moreover, at the end of every S timeslots (one period), the drones independently identify the closest charging station to recharge. Thus, each agent needs to update the state of its distances to all charging stations.

The evaluation of all algorithms includes three key metrics: 1) *Mission efficiency*, 2) *Sensing accuracy* and 3) *Energy cost*. These metrics are determined using Eq.(1), (2) and (3) respectively. We use the number of vehicles detected/observed by drones to represent the sensor data values defined in this paper. Furthermore, to obtain a comprehensive assessment that considers all three metrics, we conduct an overall performance evaluation using Eq.(4).

C. Results and Analysis

There are six dimensions for the complex scenario we study here: 1) the drones density, 2) the number of periods, 3) the number of cells, 4) the number of charging stations, 5) the density of vehicles, and 6) the number of drones with fixed density by adjusting the number of cells.

The drones density. It denotes the ratio of the number of drones over the number of cells, representing the coverage of a single drone in the map. In this case, we fix the number cells as 64, and increase the number of drones from 8 to 64, that is, the drones density increases from 0.125 to 1.0. Fig. 5 illustrates the performance of *DO-RL* and three baseline methods when using different drone densities to perform traffic monitoring. As the drones density increases, both mission efficiency and sensing accuracy of *DO-RL* increase linearly. These are approximately 23.0% and 15.8% higher than *EPOS* respectively, as shown in Fig. 5(a) and Fig. 5(b). This is because *DO-RL* controls the traveling direction of drones based on the predicted sensor data, facilitating drones to cover the area with the maximum sensing values. *MAPPO* has statistically significantly high efficiency and accuracy with a low drones density (average p-value less than 0.001), but its performance degrades when the drones density is larger than 0.375 due to the high computation complexity. In contrast, the plan selection in *DO-RL* ensures sensing fairness while reducing energy consumption, mitigating the learning difficulty caused by a large number of drones. In the energy cost in Fig. 5(c), *DO-RL* is on average 1.7% lower than *EPOS* and 7.9% lower than *MAPPO*. *Greedy* has the minimum energy cost among all methods, only 7.89% lower than *DO-RL*, but has the least performance in efficiency and accuracy. Fig. 5(d) shows that all methods except *Greedy* have similar overall performance when the drones density is 1.0, with p-value of 0.04, because there are ample drone resources available to effectively coordinate to cover the entire area.

Number of periods. As shown in Fig. 6, *DO-RL* achieves superior performance compared to other methods, increasing linearly as the number of periods increase (increased by 51.3% in quadruple time). Although it has statistically similar mission efficiency to *MAPPO* when the period is 4, this metric increases dramatically because drones update and obtain more accurate predicted sensor data with higher number of periods. The timeslot-by-timeslot learning in *MAPPO* perplexes the actions learned by drones, particularly considering that it operates with an action space thirty times larger than that of *DO-RL*, since one period has 30 timeslots. This also results in higher flying energy consumed by drones, and thus the energy cost of *MAPPO* is around 8.1% higher than *DO-RL*.

Fig. 7 illustrates the performance comparison between *DO-RL* and the three baseline methods, varying the number of cells, charging stations and the density of vehicles, while keeping the number of drones fixed at 16 and the number of periods at 8.

Number of cells. If the number of cells increases from 64 to 100, the drones density decreases. In Fig. 7(a), *DO-RL* shows a lower decrease in mission efficiency (decreased by 27.04%) than *MAPPO* (decreased by 44.50%) and *EPOS* (decreased by 45.11%) as the number of cells increases. Furthermore, *DO-RL* keeps relatively constant both sensing accuracy and energy cost as the number of cells varies.

Number of charging stations. If the number of charging stations increases from 4 to 9, drones have higher number

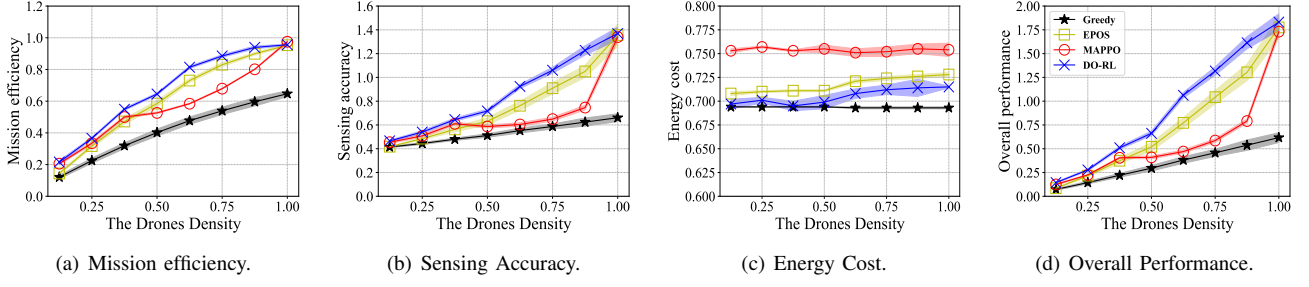


Fig. 5. **DO-RL has a higher overall performance than other methods, especially for high drones density but less than 1.** Change the drones density by increasing the number of drones from 8 to 64 and fixing 8 periods, 64 cells, 4 charging stations and high density of vehicles.

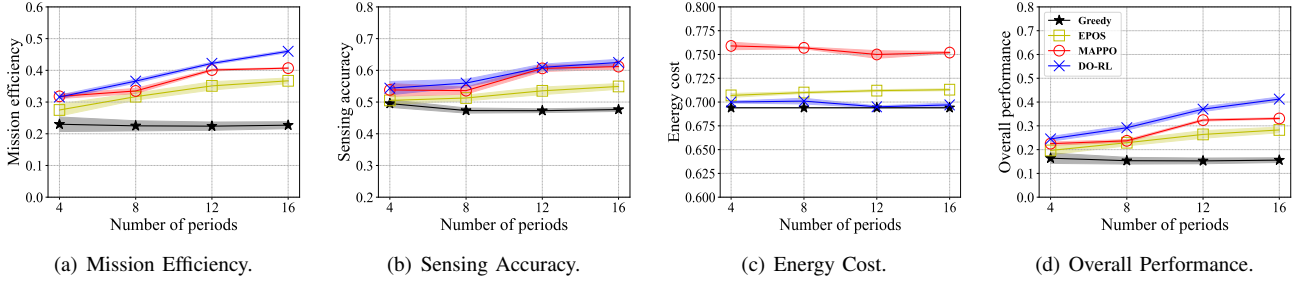


Fig. 6. **DO-RL has a higher overall performance than other methods, especially for high periods.** Change the the number of periods and fix 16 drones, 64 cells, 4 charging stations and high density of vehicles.

Scenarios	Greedy		EPOS		MAPPO		DO-RL	
	High density	Low density	High density	Low density	High density	Low density	High density	Low density
cells=64 stations=4	0.23	0.23	0.32	0.32	0.34	0.51	0.34	0.53
cells=100 stations=4	0.15	0.15	0.17	0.20	0.19	0.36	0.27	0.40
cells=64 stations=9	0.23	0.23	0.29	0.29	0.40	0.50	0.31	0.57
cells=100 stations=9	0.15	0.15	0.20	0.21	0.19	0.31	0.28	0.47

(a) Mission efficiency.

Scenarios	Greedy		EPOS		MAPPO		DO-RL	
	High density	Low density	High density	Low density	High density	Low density	High density	Low density
cells=64 stations=4	0.47	0.48	0.51	0.51	0.54	0.82	0.61	0.93
cells=100 stations=4	0.53	0.53	0.53	0.54	0.56	0.86	0.60	0.88
cells=64 stations=9	0.47	0.47	0.49	0.49	0.59	0.84	0.52	0.89
cells=100 stations=9	0.53	0.52	0.54	0.55	0.56	0.83	0.60	0.98

(b) Sensing Accuracy.

Scenarios	Greedy		EPOS		MAPPO		DO-RL	
	High density	Low density	High density	Low density	High density	Low density	High density	Low density
cells=64 stations=4	0.69	0.69	0.71	0.71	0.75	0.77	0.71	0.71
cells=100 stations=4	0.69	0.69	0.71	0.71	0.75	0.75	0.70	0.70
cells=64 stations=9	0.69	0.69	0.71	0.71	0.74	0.75	0.70	0.70
cells=100 stations=9	0.69	0.69	0.70	0.71	0.75	0.75	0.70	0.70

(c) Energy Cost.

Scenarios	Greedy		EPOS		MAPPO		DO-RL	
	High density	Low density	High density	Low density	High density	Low density	High density	Low density
cells=64 stations=4	0.16	0.17	0.23	0.23	0.24	0.55	0.29	0.69
cells=100 stations=4	0.12	0.12	0.13	0.15	0.14	0.42	0.23	0.49
cells=64 stations=9	0.16	0.16	0.20	0.20	0.32	0.56	0.23	0.72
cells=100 stations=9	0.12	0.12	0.15	0.17	0.14	0.34	0.24	0.66

(d) Overall Performance.

Fig. 7. **DO-RL is more scalable to complex sensing scenarios than other methods.** Performance comparison under varying parameters: the number of cells (64 and 100), the number of charging stations (4 and 9), and the density of vehicles.

of flying directions to choose as the number of charging stations increase, increasing the difficulty in plan selection. As a result, the overall performance of both *DO-RL* and *EPOS* decrease by 19.05% and 11.39% respectively.

Density of vehicles. If we select a new map that has low density of vehicles, the distribution of sensor data changes (with different road distribution), as shown in Fig. 4. In Fig. 7(a) and 7(b), both *DO-RL* and *MAPPO* have higher

mission efficiency and sensing accuracy than the other two methods, with average 90.65% higher efficiency and 76.85% higher accuracy. This is because the learning methods observe the environment and control drones to collect data in the cells and timeslots with the highest number of vehicles. *DO-RL* performs better than other methods in the low density of vehicles even though the number of cells and charging stations increases.

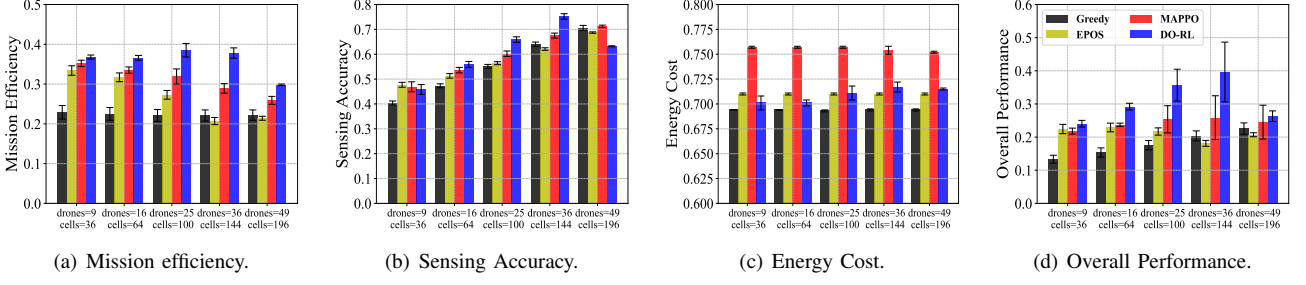


Fig. 8. **DO-RL has a higher overall performance than other methods, especially with 36 drones and 144 cells.** Change the number of drones and cells but fixing the drones density at 0.25 with 8 periods, 4 charging stations and high density of vehicles.

Number of drones/cells with fixed density. If we fix the drones density but increase the number of drones, then the number of cells increases proportionally. For example, we use the drones density in the basic scenario of 0.25, and increase the number of drones from 9 to 49 and the number of cells from 36 to 196. As shown in Fig. 8, when the number of drones/cells increases, the mission efficiency of both *EPOS* and *MAPPO* decreases (by 35.93% and 26.42% respectively). This is due to *EPOS* facing challenges in efficiently scheduling drones for a large number of cells, while *MAPPO* experiences increased computational complexity. In contrast, *DO-RL* overcomes these challenges and demonstrates a 4.62% increase in mission efficiency. When increasing to 49 drones and 196 cells, however, the overall performance of *DO-RL* degrades due to the high complexity of scheduling and computation, decreased by 33.66%. In overall, *DO-RL* has statistically higher overall performance than other methods, with an average improvement of 46.98%, which confirms the efficiency of the proposed method.

In summary, several scientific insights on experimental results are listed as follows:

- When drone resources are scarce (low drones density), it becomes more efficient and accurate to employ long-term learning methods for optimizing sensing. In contrast, when drone resources are abundant, short-term optimization methods alone suffice.
- In areas characterized by a sparse distribution of vehicles over an extended period, the DRL used by drones proves to be a more efficient and accurate approach for both learning and observing traffic flow compared to distributed optimization methods.
- The proposed method make drones energy-aware and consume less amount of energy than traditional DRL, keeping the safety of drones' batteries (more details in Appendix B).
- The proposed method's performance declines with a high number of charging stations. However, it recommends placing charging stations in vehicle-dense areas, reducing their overall number, and providing corresponding policy suggestions. (more details in Appendix B).
- The proposed method effectively combines the strengths of both DRL and distributed optimization methods and achieve high overall performance under the complex sensing environments.

VI. CONCLUSION AND FUTURE WORK

In conclusion, this paper presents a new framework named *DO-RL* to solve the decentralized sensing and recharging problem by a swarm of drones. *DO-RL* combines both short-term and long-term strategic coordination; we use distributed optimization (*EPOS*) to coordinate energy-aware drones to autonomously plan their navigation and sensing within a period, and leverage the deep reinforcement learning to schedule the flying directions of drones. Extensive experiments using simulations of urban mobility demonstrate that the *DO-RL* outperforms existing methods across various domains, including long-term sensing in resource-constrained drone environments, sparse traffic flow observation, improved energy efficiency, and optimized charging station placement. These findings highlight the substantial potential of *DO-RL* in optimizing traffic monitoring in Smart Cities.

However, the designed framework can be further improved towards several research avenues: 1) Use of state-of-the-art algorithms to extend the studies of charging scheduling and collision avoidance [40]. 2) Use of simulated and real-world datasets in other applications of Smart Cities, including free parking spots, disaster response, and smart farming. 3) Technology assessment for the real-time decentralized drone system.

ACKNOWLEDGEMENTS

This research is supported by a UKRI Future Leaders Fellowship (MR/W009560/1): *Digitally Assisted Collective Governance of Smart City Commons-ARTIO*, and the European Union, under the Grant Agreement GA101081953 attributed to the project H2OforAll—*Innovative Integrated Tools and Technologies to Protect and Treat Drinking Water from Disinfection Byproducts (DBPs)*. Views and opinions expressed are, however, those of the author(s) only and do not necessarily reflect those of the European Union. Neither the European Union nor the granting authority can be held responsible for them. Funding for the work carried out by UK beneficiaries has been provided by UK Research and Innovation (UKRI) under the UK government's Horizon Europe funding guarantee [grant number 10043071]. Thanks to Manos Chaniotakis and Zeinab Nezami for the support of transportation datasets.

REFERENCES

- [1] Tejasvi Alladi, Vinay Chamola, Nishad Sahu, and Mohsen Guizani. Applications of blockchain in unmanned aerial vehicles: A review. *Vehicular Communications*, 23:100249, 2020.
- [2] Emmanouil Barmounakis and Nikolas Geroliminis. On the new era of urban traffic monitoring with massive drone data: The pneumonia large-scale field experiment. *Transportation research part C: emerging technologies*, 111:50–71, 2020.
- [3] Daniel Hernández, Juan-Carlos Cano, Federico Silla, Carlos T Calafate, and José M Cecilia. AI-enabled autonomous drones for fast climate change crisis assessment. *IEEE Internet of Things Journal*, 9(10):7286–7297, 2021.
- [4] Godall Rohi, Godswill Ofualagba, et al. Autonomous monitoring, analysis, and countering of air pollution using environmental drones. *Heliyon*, 6(1):e03252, 2020.
- [5] Xin Li, Mooi Choo Chuah, and Subhrajit Bhattacharya. UAV assisted smart parking solution. In *2017 international conference on unmanned aircraft systems (ICUAS)*, pages 1006–1013. IEEE, 2017.
- [6] Prithvi Krishna Chittoor, Bharatiraja Chokkalingam, and Lucian Mihet-Popa. A review on UAV wireless charging: Fundamentals, applications, charging techniques and standards. *IEEE Access*, 9:69235–69266, 2021.
- [7] Sabitri Poudel and Sangman Moh. Task assignment algorithms for unmanned aerial vehicle networks: A comprehensive survey. *Vehicular Communications*, page 100469, 2022.
- [8] Jingjing Cui, Yuanwei Liu, and Arumugam Nallanathan. Multi-agent reinforcement learning-based resource allocation for UAV networks. *IEEE Transactions on Wireless Communications*, 19(2):729–743, 2019.
- [9] Ryan Lowe, Yi I Wu, Aviv Tamar, Jean Harb, OpenAI Pieter Abbeel, and Igor Mordatch. Multi-agent actor-critic for mixed cooperative-competitive environments. *Advances in neural information processing systems*, 30, 2017.
- [10] Evangelos Pournaras, Peter Pilgerstorfer, and Thomas Asikis. Decentralized collective learning for self-managed sharing economies. *ACM Transactions on Autonomous and Adaptive Systems (TAAS)*, 13(2):1–33, 2018.
- [11] Evangelos Pournaras. Collective learning: A 10-year odyssey to human-centered distributed intelligence. In *2020 IEEE International Conference on Autonomic Computing and Self-Organizing Systems (ACSOS)*, pages 205–214. IEEE, 2020.
- [12] Srijoni Majumdar, Chuhao Qin, and Evangelos Pournaras. Discrete-choice multi-agent optimization: Decentralized hard constraint satisfaction for smart cities. *International Conference on Autonomous Agents and Multiagent Systems*. Cham: Springer International Publishing, 2023.
- [13] Chuhao Qin and Evangelos Pournaras. EPOS-based Plans for Iterative Sensing and Charging. 11 2023.
- [14] Mehdi Alighanbari and Jonathan How. Robust decentralized task assignment for cooperative UAVs. In *AIAA Guidance, Navigation, and Control Conference and Exhibit*, page 6454, 2006.
- [15] Jie Chen, Xianguo Qing, Fang Ye, Kai Xiao, Kai You, and Qian Sun. Consensus-based bundle algorithm with local replanning for heterogeneous multi-UAV system in the time-sensitive and dynamic environment. *The Journal of Supercomputing*, 78(2):1712–1740, 2022.
- [16] C Qin, F Candan, L Mihaylova, and E Pournaras. 3, 2, 1, drones go! A testbed to take off UAV swarm intelligence for distributed sensing. In *Proceedings of the 2022 UK Workshop on Computational Intelligence*. Springer Nature, 2022.
- [17] Lige Ding, Dong Zhao, Mingzhe Cao, and Huadong Ma. When crowdsourcing meets unmanned vehicles: Toward cost-effective collaborative urban sensing via deep reinforcement learning. *IEEE Internet of Things Journal*, 8(15):12150–12162, 2021.
- [18] Babatunji Omoniwa, Boris Galkin, and Ivana Dusparic. Communication-enabled deep reinforcement learning to optimise energy-efficiency in UAV-assisted networks. *Vehicular Communications*, 43:100640, 2023.
- [19] Dong Zhao, Mingzhe Cao, Lige Ding, Qiaoyue Han, Yunhao Xing, and Huadong Ma. Dronesense: Leveraging drones for sustainable urban-scale sensing of open parking spaces. In *IEEE INFOCOM 2022-IEEE Conference on Computer Communications*, pages 1769–1778. IEEE, 2022.
- [20] Moataz Samir, Chadi Assi, Sanaa Sharafeddine, Dariush Ebrahimi, and Ali Ghayeb. Age of information aware trajectory planning of UAVs in intelligent transportation systems: A deep learning approach. *IEEE Transactions on Vehicular Technology*, 69(11):12382–12395, 2020.
- [21] Aakash Khochare, Yogesh Simmhan, Francesco Betti Sorbelli, and Sajal K Das. Heuristic algorithms for co-scheduling of edge analytics and routes for UAV fleet missions. In *IEEE INFOCOM 2021-IEEE Conference on Computer Communications*, pages 1–10. IEEE, 2021.
- [22] Novella Bartolini, Andrea Coletta, and Gaia Maselli. On task assignment for early target inspection in squads of aerial drones. In *2019 IEEE 39th International Conference on Distributed Computing Systems (ICDCS)*, pages 2123–2133. IEEE, 2019.
- [23] Yang Gao, Yingzhou Zhang, Shurong Zhu, and Yi Sun. Multi-UAV task allocation based on improved algorithm of multi-objective particle swarm optimization. In *2018 International Conference on Cyber-Enabled Distributed Computing and Knowledge Discovery (CyberC)*, pages 443–4437. IEEE, 2018.
- [24] Xueli Wu, Yanan Yin, Lei Xu, Xiaojing Wu, Fanhua Meng, and Ran Zhen. Multi-UAV task allocation based on improved genetic algorithm. *IEEE Access*, 9:100369–100379, 2021.
- [25] Yongbo Chen, Di Yang, and Jianqiao Yu. Multi-UAV task assignment with parameter and time-sensitive uncertainties using modified two-part wolf pack search algorithm. *IEEE Transactions on Aerospace and Electronic Systems*, 54(6):2853–2872, 2018.
- [26] Shayegan Omidshafiei, Ali-Akbar Agha-Mohammadi, Christopher Amato, Shih-Yuan Liu, Jonathan P How, and John Vian. Decentralized control of multi-robot partially observable markov decision processes using belief space macro-actions. *The International Journal of Robotics Research*, 36(2):231–258, 2017.
- [27] Chuhao Qin and Evangelos Pournaras. Coordination of drones at scale: Decentralized energy-aware swarm intelligence for spatio-temporal sensing. *Transportation Research Part C: Emerging Technologies*, 157:104387, 2023.
- [28] Da Liu, Liqian Dou, Ruilong Zhang, Xiuyun Zhang, and Qun Zong. Multi-agent reinforcement learning-based coordinated dynamic task allocation for heterogeneous UAVs. *IEEE Transactions on Vehicular Technology*, 2022.
- [29] Chi Harold Liu, Chengzhe Piao, and Jian Tang. Energy-efficient UAV crowdsensing with multiple charging stations by deep learning. In *IEEE INFOCOM 2020-IEEE Conference on Computer Communications*, pages 199–208. IEEE, 2020.
- [30] Chenxi Zhao, Junyu Liu, Min Sheng, Wei Teng, Yang Zheng, and Jiaolong Li. Multi-UAV trajectory planning for energy-efficient content coverage: A decentralized learning-based approach. *IEEE Journal on Selected Areas in Communications*, 39(10):3193–3207, 2021.
- [31] Mouna Elloumi, Riadh Dhaou, Benoit Escrig, Hanen Idoudi, and Leila Azouz Saidane. Monitoring road traffic with a UAV-based system. In *2018 IEEE Wireless Communications and Networking Conference (WCNC)*, pages 1–6. IEEE, 2018.
- [32] Hailong Huang, Andrey V Savkin, and Chao Huang. Decentralized autonomous navigation of a UAV network for road traffic monitoring. *IEEE Transactions on Aerospace and Electronic Systems*, 57(4):2558–2564, 2021.
- [33] David Castells-Graells, Christopher Salahub, and Evangelos Pournaras. On cycling risk and discomfort: urban safety mapping and bike route recommendations. *Computing*, 102:1259–1274, 2020.
- [34] Joshua K Stolaroff, Constantine Samaras, Emma R O’Neill, Alia Lubers, Alexandra S Mitchell, and Daniel Ceperley. Energy use and life cycle greenhouse gas emissions of drones for commercial package delivery. *Nature communications*, 9(1):409, 2018.
- [35] Evangelos Pournaras, Srivatsan Yadhunathan, and Ada Diaconescu. Holographic structures for decentralized deep learning: a performance analysis. *Cluster Computing*, 23(1):219–240, 2020.
- [36] John Schulman, Filip Wolski, Prafulla Dhariwal, Alec Radford, and Oleg Klimov. Proximal policy optimization algorithms, 2017.
- [37] Company DJI. DJI Phantom 4 Pro. <https://www.dji.com/uk/phantom-4-pro/info#specs>. Accessed: 2022-11-16.
- [38] Damian Wierzbicki. Multi-camera imaging system for UAV photogrammetry. *Sensors*, 18(8):2433, 2018.
- [39] Evangelos Pournaras. Multi-level reconfigurable self-organization in overlay services. 2013.
- [40] Fethi Candan. A comparison of obstacle dependent gaussian and hybrid potential field methods for collision avoidance in multi-agent systems. *Manchester Journal of Artificial Intelligence and Applied Sciences*, 2(1), 2021.

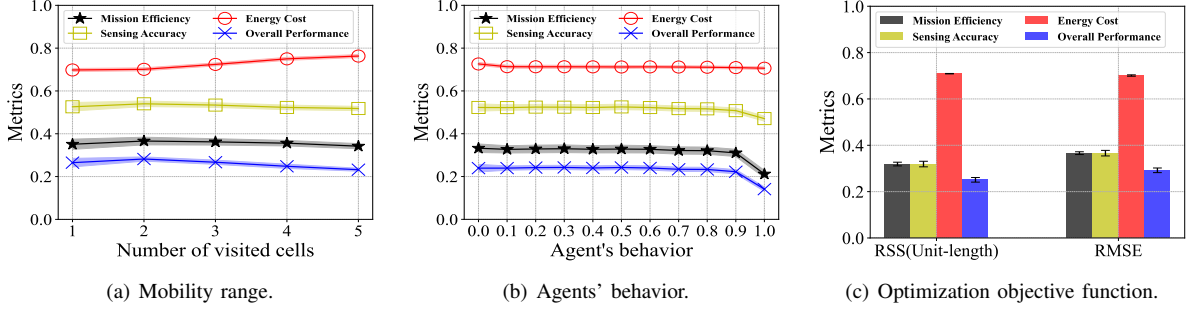


Fig. 9. *DO-RL* has a superior overall performance when $J_u = 2$, $\beta \in [0.1, 0.8]$, and using RMSE. Change the parameters of the proposed method in mobility range, agents' behavior and optimization objective function.

APPENDIX A EFFECT OF DIFFERENT PARAMETERS

The objective of this appendix is to analyze the impact of various parameters within the plan generation and distributed optimization of the proposed method. The insights derived from this appendix guide us in making informed empirical decisions regarding parameter selection for the evaluation scenarios. While the calculations presented herein can be automated for any scenario during hyper-parameter optimization. Such optimization is not the focus of this paper.

We use the *DO-RL* and the basic scenario to test the mobility range, the agents' behavior, and the objective function of optimization.

Mobility range. Fig. 9(a) illustrates the effect of different numbers of visited cells. The higher the number of cells a drone visits, the higher the flying energy is, and the higher the energy cost is. The high number of visited cells perplexes the spatio-temporal navigation and sensing of a drone, leading to the over-sensing. Specifically, multiple drones visit the same cell simultaneously and waste energy on collecting the same data. In contrast, if drones visit only one cell, they are free from over-sensing, but have a high probability to miss the area with a high required sensing data due to its low mobility range. As a result, we empirically select $J^u = 2$ for each drone to optimize the overall performance.

Agents' behavior. Fig. 9(b) illustrates the effect of agents' behavior by varying the parameter of β [10]. As β increases from 0 to 1, agents reduce the energy cost of their selected plans, while decreasing both efficiency and accuracy. This is because, according to Eq. 5, drones with higher β choose a plan with lower energy cost, and degrades the matching between the total sensing and the target. Since the overall performance when $\beta \in [0.1, 0.8]$ are statistically similar, with p-value of 0.0003 on average, drones are allowed to choose their behaviors within this range.

Optimization objective function. Fig. 9(c) illustrates the comparison of two different optimization objective function used in EPOS. Apart from RMSE, we choose the correlation error, i.e., the residual sum of squares (RSS) between the aggregated plans and the target, both in unit-length scaled. The results show that RSS has statistically lower

efficiency and accuracy, and thus has statistically lower overall performance than RMSE (p-value less than 0.001). This is because the result of RSS is significantly higher than RMSE. Therefore, drones choose the higher agents' behaviors, disrupting the matching between the total sensing and the target.

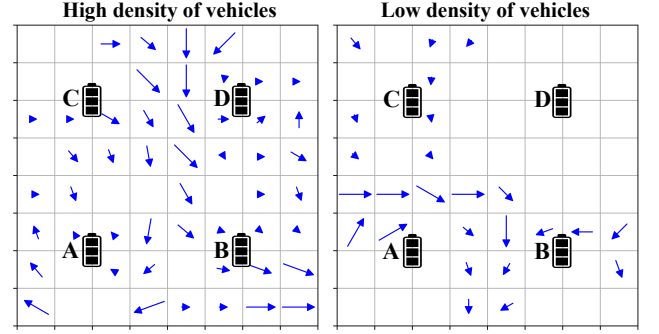


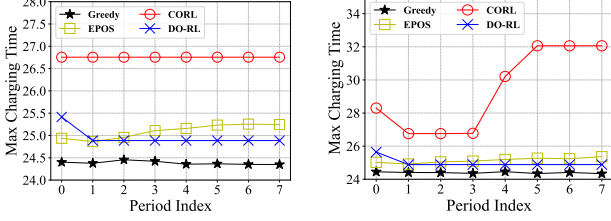
Fig. 10. The distribution of both charging stations and traffic vehicles in the maps with high and low density of vehicles. There are 4 charging stations uniformly distributed in the map with $64 = 8 \times 8$ cells lined up over the map. The blue arrows symbolize the flow of vehicular traffic, with their length proportional to the volume of vehicles over 8 periods.

APPENDIX B EVALUATION ON THE CHARGING

In this appendix, we use the proposed *DO-RL* and the baseline methods to study the followings:

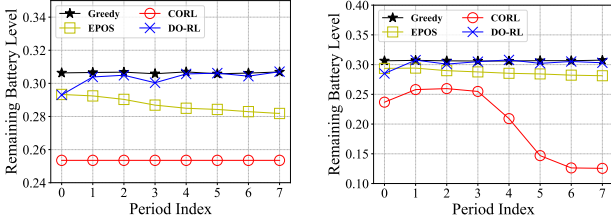
- **Max charging time.** It is the longest charging time consumed by drones at each time period. It is calculated by a drone's required energy for charging divided by the charging power. This aims to provide drones with sufficient charging time such that they can depart simultaneously at the next time period.
- **Remaining battery level.** It denotes a percentage of battery level once drones have completed their sensing tasks. The value is calculated as an average among all drones within each time period. Its purpose is to determine if each drone possesses a sufficient battery reserve for safe operation.
- **Charging load.** It is the total energy demand of drones on each charging station over all time periods. This aims to study the placement of charging stations.

We vary the scenarios to evaluate the charging in the density of vehicles based on the basic scenario (16 drones, 8 periods, 4 charging stations and 64 cells). Fig. 10 shows the distribution of both charging stations and traffic vehicles in the map.



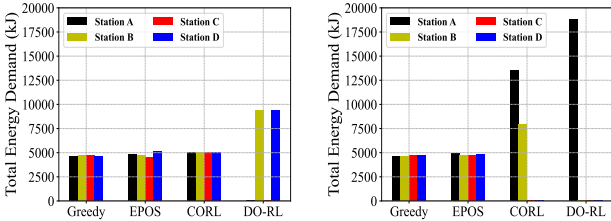
(a) Max charging time, high density of vehicles. (b) Max charging time, low density of vehicles.

Fig. 11. **DO-RL requires at least 26.3min charging time.** Performance comparison of the maximum charging time of four methods on both high and low density of vehicles.

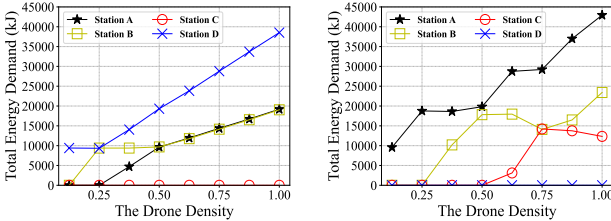


(a) High density of vehicles. (b) Low density of vehicles.

Fig. 12. **DO-RL keeps drones at a safe remaining battery level.** Performance comparison of the remaining battery level of four methods on both high and low density of vehicles.



(a) Drones density=0.25, high density of vehicles. (b) Drones density=0.25, low density of vehicles.



(c) drones density for DO-RL, high density of vehicles. (d) drones density for DO-RL, low density of vehicles.

Fig. 13. **DO-RL relies on a smaller number of charging places compared to other methods.** Performance comparisons of the total energy demand of four methods with 0.25 drones density (a and b), and the DO-RL with different drones density (c and d). Both comparison are categorized by the high and low density of vehicles.

Max charging time. The charging efficiency for the drone is 100 watt per second. As shown in the Fig. 11(a) and 11(b), *DO-RL* has the maximum charging time of 26.3min over 8 periods, which is on average 1.46% lower than *EPOS* and 6.99% lower than *MAPPO* respectively, only 2.17% higher than *Greedy*. Due to the high energy cost for sensing missions, *MAPPO* requires the highest charging time for drones, even overpass 30min in low density of vehicles. As a consequence, the proposed *DO-RL* requires no more than 30min for drones charging. To ensure all drones have sufficient charging time and depart simultaneously at the next time period without delaying, the minimum charging period can be set as 30min.

Remaining battery level. As shown in the Fig. 12(a) and 12(b), *DO-RL* keeps drones at a high remaining battery level on high and low density of vehicles, with approximately 30.25% and only 1.05% lower than *Greedy*. This level follows the drones' safety regulations which suggest finishing the missions when battery life is around 25% – 30%. However, *MAPPO* disobeys the regulations in low density of vehicles, and the minimum battery level can reach 12.55%.

Charging load. As shown in the Fig. 13(a) and 13(b), the total energy demand on charging stations of *DO-RL* over all periods is more imbalanced compared to other methods. This is because with *DO-RL* drones learn to travel to the areas with the high required sensing data values. Since drones set the nearest charging stations as destinations, they reply on a small number of charging places. For example, as shown in Fig. 13(c) and 13(d), when the drones density is 0.125 in high density of vehicles, drones only depart from and return to the charging station *D* since the vehicle distribution around *D* is more dense than other charging stations. As the drones density becomes 1, drones gradually rely on the charging station *B* and *D*. Similarly, drones only need to fly over the vehicle-dense areas around the charging station *A* and *B* in low density of vehicles. These results suggest policy for building more number of charging stations on the vehicle-dense areas to support the charging of drones.